CrossMark

Capturing Non-equilibrium Effects of Micro/Nano Scale Gaseous Flow Using a Novel Lattice Boltzmann Model

Ali Norouzi[1] · Javad Abolfazli Esfahani[1]

Abstract In this study, gaseous flow through a micro/nano-channel is investigated via a novel two relaxation time lattice Boltzmann method. In this method, the slip velocity at the fluid-solid interface is realized by defining the free relaxation parameter. Furthermore, in order to capture the non-linear phenomena associated with the Knudsen layer, the wall function correction is employed. To this respect, different available wall functions are implemented. The objective of the study is to provide a comparative study on the accuracy, range of applicability and computational efficiency of these wall functions in a wide range of Knudsen numbers. The results of the present study are compared against direct simulation Mont Carlo and information preservation data. It is found that only a few of the implemented wall functions are capable of predicting the flow behavior with reasonable accuracy, particularly when the Knudsen number lies in the transition flow regime.

Keywords Micro/nano-channel · Two relaxation time lattice Boltzmann method · Knudsen layer · Wall function

1 Introduction

According to the increasing interest in development of micro/nano-fabricated devices in recent years, the study of rarefied gas dynamics becomes an appealing field of research in fluid mechanics. It has been demonstrated that the Boltzmann equation can accurately describe the basic physics of such micro/nano-flows. However, the complicated form of the

✉ Javad Abolfazli Esfahani
abolfazl@um.ac.ir; jaesfahani@gmail.com

Ali Norouzi
ali.norouzi@stu.um.ac.ir

[1] Center of Excellence on Modelling and Control Systems, (CEMCS) & Department of Mechanical Engineering, Faculty of Engineering, Ferdowsi University of Mashhad, P.O. Box: 91775-1111, Mashhad, Iran

collision operator in the Boltzmann equation makes it extremely difficult to solve the equation using the available numerical methods.

On the other hand, the behavior of micro/nano-scale flows can successfully be described using the direct simulation Monte Carlo (DSMC) method. However, this is also computationally expensive and impractical for many three dimensional systems, particularly in the low Mach number limit.

The lattice Boltzmann method (LBM) is an alternative tool for simulation of rarefied gas flows. Although, this method is originated from the lattice gas automata (LGA), it can be viewed as a special discretization scheme for the Boltzmann equation [1,2]. However, it has been criticized that most of the available lattice Boltzmann models are insufficient for prediction of finite Knudsen number flows. The reason for this deficiency lies in the fact that the standard LBM, which generally works at the Navier–Stokes level, does not necessarily converge to the Boltzmann equation, particularly at high Knudsen numbers. Therefore, several efforts have been devoted to extend the validity of LBM to high Knudsen number flows by developing higher orders of the lattice Boltzmann equation (LBE) [1,3–6]. The main idea behind this approach is that by employing higher orders of the Gauss-Hermite quadrature (a finer set of discrete velocity space) and retaining higher order terms of the Hermite expansion, the LBM will converge to the Boltzmann equation. However, in practice, there are several barriers against developing the higher order LBM for capturing non-equilibrium effects of rarefied gas flows. For instance, it is found that the discrete velocities of the high-order models of LBM may not match the lattice nodes and consequently, the computational efficiency and simple algorithm of LBM cannot be guaranteed in such a situation [1,7]. Moreover, it has been demonstrated that the accuracy of results does not necessarily increase by implementing a finer set of discrete velocities [4]. This means that, there is no guarantee that by implementing a finer set of discrete velocities, the corresponding LBM leads to more accurate predictions. Therefore, introducing a general higher order LBM, which can provide accurate predictions with reasonable computational efficiency over a wide range of Knudsen numbers, is still a challenging issue in the field.

The second choice for capturing the Knudsen layer phenomena using the LBM is to employ wall distance functions. In this approach, an external expression will be implemented in order to model the effect of solid walls on the mean free path (MFP) of the gas. In this approach, the main challenging issue is obtaining an appropriate expression, which is capable of predicting the variation of the free path in the Knudsen layer region. Using wall distance functions was first proposed by Zhang et al. [8] in order to extend the validity of the continuum based LBM into high Knudsen numbers. They developed a formula for the reduction of MFP due to gas-wall interactions. Based on the classical theory of probability density, which was proposed by Stops [9] and by using a second order slip velocity model, Guo et al. [10] investigated rarefied gas flows bounded by two parallel plates in the transition regime. According to this model, Xu and Guo [11] investigate the effect of rarefaction level, pressure ratio and aspect ratio on the pressure distribution along a micro-channel in the slip and transition regimes. On the other hand, Arlemark et al. [12] derived an effective MFP expression by using the integrated form of the probability distribution function, which is relatively easy to implement in comparison with Stops original expression. More recently, Dongari et al. [13] proposed a power law based effective MFP for flows confined between two planar plains by considering the boundary limiting effects on the free path of molecules. They claimed that the new function covers a wider range of Knudsen numbers in comparison with previous models. They further developed a new power law model which is capable of describing the effect of curved surfaces on the effective MFP of the rarefied gas flows. The feasibility of this model is

also examined for the isothermal rarefied gas flow confined between two concentric rotating cylinders [14].

It is also worth noting that some studies attempt to extend the validity of the continuum based methods into the transition flow regime by introducing the effective viscosity term as a function of the Knudsen number. This approach is mainly based on the effective viscosity proposed by Karniadakis et al. [15]. In this context, Shokouhmand and Isfahani [16] showed that modifying the viscosity using the expression of Karniadakis et al. [15] improves the prediction of rarefied gas flows to some extent. Li et al. [17] employed a Bosanquet-type effective viscosity obtained by Michalis et al. [18] in order to consider the effect of rarefaction on the fluid viscosity. In general, the effective MFP obtained by using wall functions depends on the normal distance from the wall, while these effective viscosity correlations are independent of the distance from the wall because they are averaged over the cross section of the corresponding geometry. In the context of the effective viscosity, several other expressions are also proposed from different viewpoints [19,20]. These expressions can be implemented along with different continuum based methods in order to study high Knudsen number flows. However, these models mainly employ fitting data on the Boltzmann equation solution, which can limit their applications [14]. Another approach is introduced by Toschi and Succi [21] in order to study rarefied gas flows using hydrodynamics models such as the D2Q9 LBE. They introduced a virtual wall collision model to limit the runaway behavior of particles at high Knudsen numbers. Numerical results show that this approach is able to capture the gas flow behavior in micro-channels at moderate Knudsen numbers.

Another important issue associated with micro/nano-gas flow simulations using LBM is how to choose the appropriate lattice Boltzmann model. In general, LBM can be classified into single relaxation time (SRT) and multiple relaxation time (MRT) models. For most of fluid dynamics problems the choice of SRT or MRT makes a negligible difference in the final results. However, it is criticized that LBM with only one relaxation time might not be a reliable method for investigation of rarefied gas flows, since this model suffers from numerical artifacts associated with boundary conditions [22–24]. For instance, in [24] it is shown that the slip velocity obtained by the SRT-LBE includes an error term related to the grid resolution. In other words, it is observed that a part of slip velocity predicted by SRT-LBE using Bhatnagar–Gross–Krook collision model is due to numerical artifacts. This deficiency leads to incorrect results even in simple rarefied gas flow simulations. Furthermore, this error becomes more significant as the Knudsen number increases [24]. Consequently, simulation of rarefied gas flows using the standard SRT-LBE model is questionable. To overcome this deficiency, MRT model has been successfully implemented [11,25,26]. However, this model is computationally more complicated than the SRT model.

Recently, we demonstrated that LBE with two relaxation times (TRT) is a potential tool for investigation of finite Knudsen number flows [27]. It has been found that by defining the free relaxation parameter, TRT model can appropriately overcome the deficiencies of the SRT model. In a separate study, we proposed a generalized TRT model based on the wall function approach, which can satisfactorily predict micro/nano-gas flows in the slip and transition flow regimes [28]. It is also shown by a test case that while the difference between TRT and MRT results is less than 1 %, the computational run time of TRT is significantly lower than MRT code. Therefore, TRT-LBE provides great potential for investigating rarefied gas flows.

As it is mentioned above, several studies of LBM have been devoted to study micro/nano-scale gas flows using the wall function approach. It is found that this approach is capable of describing the rarefied gas flow behavior in the transition regime. However, the lack of information about the applicability, accuracy and computational efficiency of these wall functions has motivated the present study to compare the available wall functions from

different viewpoints. To this respect, the general TRT model developed in our previous work [28] is employed in order to investigate the gas flow behavior in a micro/nano-channel by using various wall function relations. Some of the considered wall functions are implemented for the first time in the framework of the lattice Boltzmann method, while the others have been implemented using SRT or MRT models in previous studies of the LBM [8,26,29,30]. The accuracy of results is evaluated with respect to the available published data in a wide range of Knudsen numbers.

2 TRT-LBE

Recently, Norouzi and Esfahani [28] demonstrated that LBE with two relaxation times can be a promising method for modeling of finite Knudsen number flows. Accordingly, we employ this model in order to simulate micro/nano-channel flows in the present study. The general form of the TRT-LBE can be expressed as follows:

$$f_i(x + e_i \delta t, t + \delta t) - f(x, t) = \Lambda(f_i) \tag{1}$$

where f_i, x, t, δt and e_i are the particle distribution function, position, time, time step and discrete velocity, respectively. The collision operator in the TRT model can be defined as [31]:

$$\Lambda = \frac{(n^s - f^s)}{\tau_s} + \frac{(n^a - f^a)}{\tau_a} \tag{2}$$

where n is the equilibrium distribution function, τ is the relaxation time which will be defined later and letters s and a represent the symmetric and anti-symmetric parts of the collision process, respectively. The fluid density and velocity can be calculated as:

$$\rho = \sum f_i \tag{3a}$$

$$u = \frac{1}{\rho} \sum e_i f_i \tag{3b}$$

In this study the D2Q9 system is employed, in which the equilibrium distribution function can be written as:

$$n_i = \rho \omega_i \left[1 + 3e_i . u + \frac{9}{2}(e_i . u)^2 - \frac{3}{2} u^2 \right] \tag{4}$$

where $\omega_0 = 4/9$, $\omega_i = 1/9 (i = 1 - 4)$ and $\omega_i = 1/36$ $(i = 5 - 8)$ are the corresponding weight coefficients related to the velocity e_i. The symmetric and anti-symmetric parts of the particle distribution function can be expressed by:

$$f_i^s = \frac{1}{2}(f_i + f_{\bar{i}}) \tag{5a}$$

$$f_i^a = \frac{1}{2}(f_i - f_{\bar{i}}) \tag{5b}$$

where $\bar{i}$ is the direction opposite to i. The fluid viscosity can also be obtained as follows:

$$v = c_s^2 \left(\tau^s - \frac{1}{2} \right) \delta t \tag{6}$$

where $c_s = RT$ is the sound speed, in which R and T denote the universal gas constant and temperature, respectively. Pressure can also be computed by an equation of state as follows:

$$P = c_s^2 \rho \tag{7}$$

Fig. 1 Geometry of Poiseuille
gas flow through two parallel
plates with height H and length L
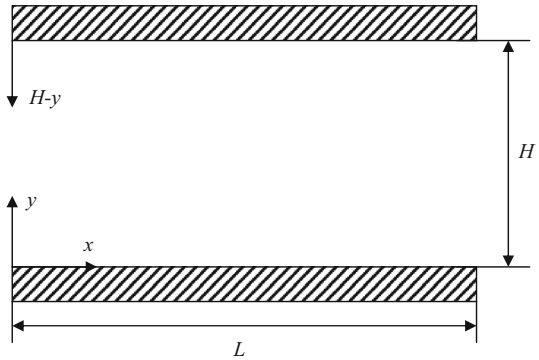
3 Wall Function Implementation

As the Knudsen number increases, the non-equilibrium effects of the Knudsen layer, which
are usually ignored in the continuum regime, start to dominate the gas flow behavior [32].
Consequently, in order to simulate rarefied gas flows in the transition regime, the Knudsen
layer must be captured properly. However, it has been demonstrated that the standard LBM,
which is mainly developed for solving the Navier–Stokes equations at the hydrodynamics
level, fail to work in such situations. In the present study, the wall function technique is
employed in order to overcome this difficulty. Accordingly, the value of effective MFP will
be defined by the following expression:

$$\lambda_e = \lambda \psi(y, Kn) \tag{8}$$

where λ and ψ are the gas MFP and wall function correction, respectively and y is the
distance from the lower wall (see Fig. 1). In this context, Zhang et al. [8] proposed the
following geometry dependent wall function for flows through micro/nano-channels:

$$\psi(y, Kn) = \frac{1}{1 + 0.7\left[\exp(-Cy/\lambda) + \exp(-C(H - y)/\lambda)\right]} \tag{9}$$

where $C = 1$ is obtained from the Kramers' problem [8]. This model is recognized as ψ_1
in the present study. Guo et al. [33] proposed another relation, in which the wall function is
only dependent on the Knudsen number and not on the distance from the wall boundaries:

$$\psi(Kn) = \frac{2}{\pi} \arctan\left(\sqrt{2}Kn^{-3/4}\right) \tag{10}$$

This expression states that the wall function is averaged over the cross section of the channel.
Here, the term ψ_2 is used to specify this model. Stops derived an exponential wall distance
function by using the solid angle analysis, which can be written as [9]:

$$\begin{aligned}
\psi(y, Kn) = \ & \frac{1}{2}\left[2 + \left(\frac{y}{\lambda} - 1\right)\exp\left(-\frac{y}{\lambda}\right) - \left(\frac{y}{\lambda}\right)^2 Ei\left(\frac{y}{\lambda}\right)\right. \\
& \left. + \left(\frac{H - y}{\lambda} - 1\right)\exp\left(-\frac{H - y}{\lambda}\right) - \left(\frac{H - y}{\lambda}\right)^2 Ei\left(\frac{H - y}{\lambda}\right)\right]
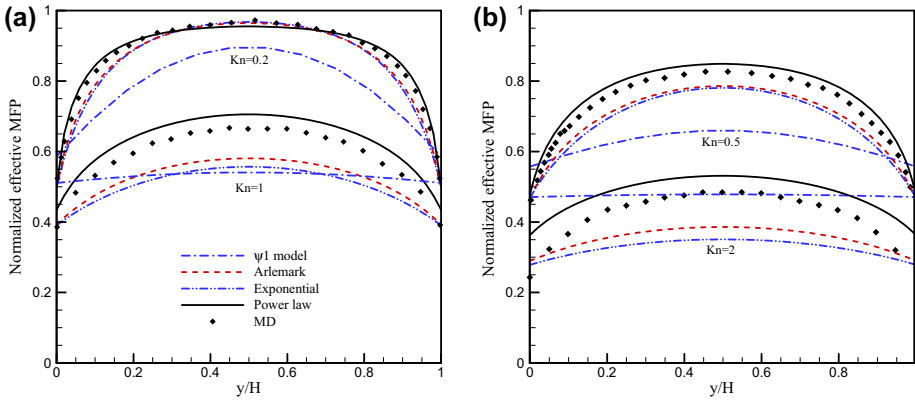\end{aligned} \tag{11}$$

Fig. 2 Functional behavior of normalized effective MFP for different Knudsen numbers. Comparison of wall functions with MD data [34]. **a** Kn = 0.2 and 1, **b** Kn = 0.5 and 2

It should be noted that the exponential integral function Ei in the above expression has been proved to be difficult to calculate using either analytical or numerical methods. Alternatively, Arlemark et al. [12] proposed another relation based on the integrated form of the probability distribution function using Simpson's numerical integral method, which can be written as a simple series function:

$$\psi(y, Kn) = 1 - \frac{1}{82} \left[\begin{array}{l} \exp\left(-\frac{y}{\lambda}\right) + \exp\left(-\frac{H-y}{\lambda}\right) + 4 \sum_{i=1}^{7} \exp\left(-\frac{y}{\lambda \cos\left[\frac{(2i-1)\pi}{28}\right]}\right) \\ + 4 \sum_{i=1}^{7} \exp\left(-\frac{H-y}{\lambda \cos\left[\frac{(2i-1)\pi}{28}\right]}\right) + 2 \sum_{i=1}^{6} \exp\left(-\frac{y}{\lambda \cos\left[\frac{\pi i}{14}\right]}\right) \\ + 2 \sum_{i=1}^{6} \exp\left(-\frac{H-y}{\lambda \cos\left[\frac{\pi i}{14}\right]}\right) \end{array} \right] \quad (12)$$

Following the same idea, Dongari et al. [13] claimed that a power law based wall function can describe the effect of solid surfaces on the effective MFP more accurately. Accordingly, they proposed an expression for gas molecules confide by two planar planes as follows [13]:

$$\psi(y, Kn) = 1 - \frac{1}{96} \left[\begin{array}{l} \left(1 + \frac{r}{\lambda}\right)^{-2} + \left(1 + \frac{H-r}{\lambda}\right)^{-2} + 4 \sum_{i=1}^{8} \left(1 + \frac{r}{\lambda \cos\left[\frac{(2i-1)\pi}{32}\right]}\right)^{-2} \\ + 4 \sum_{i=1}^{8} \left(1 + \frac{H-r}{\lambda \cos\left[\frac{(2i-1)\pi}{32}\right]}\right)^{-2} + 2 \sum_{i=1}^{7} \left(1 + \frac{r}{\lambda \cos\left[\frac{i\pi}{16}\right]}\right)^{-2} \\ + 2 \sum_{i=1}^{7} \left(1 + \frac{H-r}{\lambda \cos\left[\frac{i\pi}{16}\right]}\right)^{-2} \end{array} \right] \quad (13)$$

In this section, the behavior of the considered wall functions (ψ_1, Arlemark, exponential and power law models) is investigated for different Knudsen numbers. For this reason, the variation of normalized effective MFP (i.e., λ_e/λ) is plotted along the cross section of the channel for different Knudsen numbers. Figure 2a represents the results for Kn = 0.2 and 1 and Fig. 2b is obtained for Kn = 0.5 and 2. In order to evaluate the accuracy of these wall functions, the molecular dynamics (MD) data of Dongari et al. [34] is employed in this study. As can be seen, at low Knudsen numbers (Kn = 0.2), the Knudsen layer only affects the near wall region. As the Knudsen number increases, the Knudsen layer spreads into the

bulk region of the flow field as well. It can also be observed that ψ_1 model is incapable of following the correct trend even at low Knudsen numbers. This deficiency can be attributed to the fact that this model is originally obtained for the Kramers' problem and therefore, it cannot provide accurate predictions for Poiseuille gas flows in micro/nano-channels, particularly as the Knudsen number increases in the transition regime. When Kn = 0.2, all of the considered wall functions except ψ_1 model are in good agreement with MD data [34], but the power law model provides the best prediction in the near wall region at this level of rarefaction. For Kn = 0.5 and 1, the power law model still presents the most accurate results among the considered relations, although it over predicts the value of the MFP, particularly in the bulk region. Finally, at Kn = 2 when the rarefaction effects dominate the flow behavior, the power law model significantly over predicts the effective MFP in the near wall region as well as the bulk region. However, the exponential and Arlemark models provide better predictions in the near wall region, although they significantly underestimate the value of MFP far away from the walls.

4 Boundary Conditions

Several slip schemes have been developed to capture the slip velocity at the wall using the lattice Boltzmann model. The diffuse scattering [35], diffuse-bounce back [24] and bounce back-specular [36] boundary conditions are the most representative ones. In this study, we implement the method proposed in [28] in order to realize the slip velocity at the wall. In this method the bounce back boundary condition is applied to the walls of the channel and the slip velocity is realized by defining an effective anti-symmetric relaxation time. It has been demonstrated that this method can appropriately eliminate the artifacts in prediction of slip velocity at the wall, if the relaxation parameters are defined properly [28]. On the other hand, this method utilizes the standard bounce back at the solid nodes. Therefore, there is no need to implement the combination factor, which is mainly used in the diffuse-bounce back and bounce back-specular boundary conditions, in order to specify the portion of particles that reflects specularly or diffusively when they hit the wall [37]. Consequently, this approach can achieve faster computational performance and it can provide better numerical stability as well. In this method, the second order slip velocity model is employed in order to derive the effective anti-symmetric relaxation time as follows [28]:

$$\tau^a = \left[\frac{\sqrt{6\pi} H (A_1 + 2A_2 Kn_e)}{8} + \frac{8\tau^s - 1}{16\tau^s - 8} \right] \tag{14}$$

where $Kn_e = \psi Kn$ is the effective Knudsen number. It should be noted that the Knudsen number varies across the length of the channel as follows:

$$Kn = \frac{Kn_o P_o}{P(x)} \tag{15}$$

where, Kn_o and P_o are the Knudsen number and pressure at the outlet of the channel [30]. Also, A_1 and A_2 are the coefficients of the second order slip velocity model which are given by:

$$A_1 = \frac{2 - \sigma}{\sigma} (1 - 0.1817\sigma) \tag{16a}$$

$$A_2 = \frac{1}{\pi} + \frac{A_1^2}{2} \tag{16b}$$

in which $\sigma = 1$ is the tangential accommodation coefficient.

The symmetric relaxation time is also a function of Knudsen number as follows [27,30]:

$$\tau^s = \frac{1}{2} + \sqrt{\frac{6}{\pi}} K n_e H \tag{17}$$

Therefore, the relaxation time becomes a function of the gas MFP as follows:

$$\tau^s = \frac{1}{2} + \sqrt{\frac{6}{\pi}} \psi \times \lambda \tag{18}$$

The average pressure boundary condition is imposed at the inlet and outlet of the channel by using the extrapolation scheme introduced in [24].

5 Results and Discussion

In this part, some numerical results for the gas flow in a micro/nano-channel are presented. A grid independence study is performed to determine the appropriate grid resolution. Accordingly, the grid size $N_x \times N_y = 1100 \times 11$ is utilized in all simulations, unless otherwise stated. Furthermore, in all cases, the Mach number is lower than 0.043 which satisfies the low Mach number assumption of the LBM.

The velocity profiles normalized by the average velocity U_{ave} are given in Fig. 3. Here, the constant pressure boundary condition is applied to the inlet and outlet of the channel with the pressure ratio $P_{in}/P_{out} = 2$ and the DSMC solution [15] is employed in order to evaluated the accuracy of the present LBE model using various wall distance functions. As can be seen, at the early transition flow regime (Fig. 3a), the velocity profiles of all models are almost similar and the wall function correction plays a negligible role in the near wall region. In this case, the LBE without using wall function correction can satisfactorily present the velocity slip at the wall. As the Knudsen number increases, the deviation between different models becomes remarkable. For instance, at Kn = 1 (Fig. 3b) ψ_1 and ψ_2 models significantly over predict the slip velocity at the wall and under predict the maximum velocity at the centerline of the channel, although they still provide better predictions rather than the standard TRT model without using wall function corrections. On the other hand, the more sophisticated models (i.e., power law, Arlemark and exponential models) remain relatively accurate at this Knudsen number. For Kn = 5 (Fig. 3c) the power law, Arlemark and exponential models over predict the slip velocity at the wall and under predict the maximum velocity at the centerline of the channel. However, they can significantly improve the accuracy of velocity profiles in comparison with the standard TRT-LBE without using wall functions. In contrast, ψ_1 model and the LBE without using wall functions fail to work at Kn = 5. At the upper bound of the transition regime (Fig. 3d), the exponential, Arlemark and power low functions can still capture the Knudsen layer effects reasonably. However, the results deviate from those obtained by DSMC method, particularly in the near wall region. The differences of slip velocities obtained by the present LBE using the exponential, power law and Arlemark models with those obtained by DSMC method for Kn = 10 are about 4.25, 4.98 and 5.02 %, respectively. It is evident that the exponential relation is in a slight better agreement with DSMC results at the channel walls. On the other hand, the agreement between the centerline velocity predicted by these wall functions and those obtained by DSMC method deteriorates as the Knudsen number exceeds 5. It should be pointed out that the present LBE model using ψ_1 correction function and also without using wall functions encounters some numerical
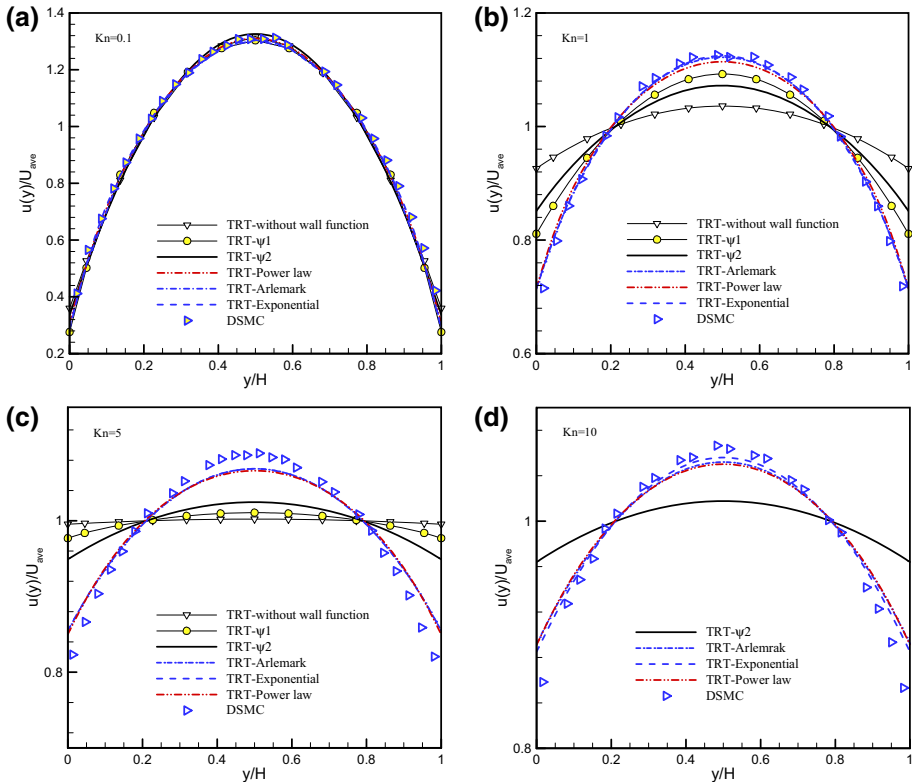
Fig. 3 Comparison of the present TRT-LBE velocity profiles using different wall functions with DSMC results [15] at different Knudsen numbers

instabilities for Kn = 10 and therefore, it cannot produce reasonable results. In order to overcome this deficiency, a more robust initial condition may be helpful.

The above comparison clearly reveals that the wall function corrections, which are based on the probability distribution function (i.e., exponential, Arlemark and power law models), can significantly improve the prediction of velocity profiles in the transition flow regime. However, the other models (i.e., ψ_1 and ψ_2 models) work only at the early transition flow regime. Similarly, in Zhang et al. [8] it is reported that ψ_1 model provides an improvement in the LBE predictions up to Kn $\sim$ 0.5. This conclusion is in agreement with the present observations.

In order to investigate the performance of the wall functions in prediction of flow behavior, the normalized mass flow rate, which is defined as $\bar{m} = 2\dot{m}/(\rho_{ave}\sqrt{2RT})$, where ρ_{ave} is the average density between the inlet and outlet, is plotted against the inlet Knudsen number. The results are presented for a channel with aspect ratio 20 and pressure ratio 10/7 in order to compare them against the IP-DSMC data [38]. As can be seen from Fig. 4, the standard LBE model is incapable of describing the mass flow behavior for Knudsen numbers higher than 0.4. Furthermore, the LBE using ψ_1 model can appropriately capture the Knudsen minimum phenomenon, but it fails to work for Kn > 1. On the other hand, ψ_2 and power law models over predict the mass flow rate value in comparison with the IP data when the Knudsen number

Fig. 4 Variation of normalized mass flux against inlet Knudsen number. Comparison of IP-DSMC results [38] with TRT-LBE using various wall function models
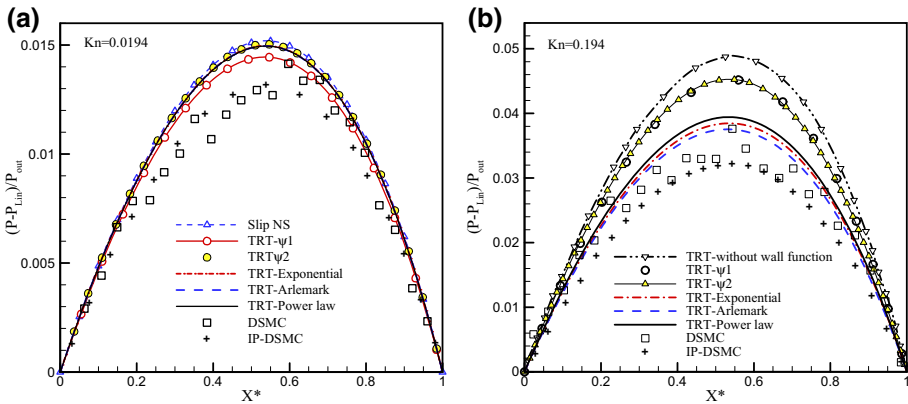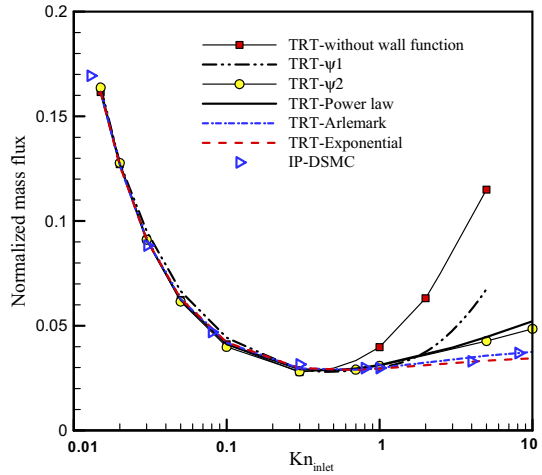

Fig. 5 Pressure deviation from the linear pressure for outlet Knudsen numbers of 0.0194 and 0.194. Comparison between DSMC and IP results (Data taken from [24]) with present TRT-LBE using different wall functions

exceeds 1. Another important key point is that the present TRT-LBE using the exponential and Arlemark expressions remains in quite good agreement with the IP solution up to Kn = 10.

Pressure deviation from the linear pressure is recognized as one of the important features of gas flows through micro/nano-channels. Figure 5 illustrates the variation of this parameter across the length of the channel for outlet Knudsen numbers of 0.0194 and 0.194. Here, P_{Lin} denotes the linear pressure distribution between the inlet and outlet of the channel and normalized length is defined as $X* = x/L$, where L is the total length of the channel. It is noted that in this part, the grid resolution 2100×21 is utilized. As can be seen, for Kn = 0.0194, which is in the slip flow regime, TRT-LBE using the exponential, Arlemark, power law and ψ_2 wall functions slightly over predict the maximum pressure deviation in comparison with that of the DSMC method. On the other hand, ψ_1 model is in good agreement with the DSMC data. Furthermore, the results of the present TRT-LBE model agree well with the analytical solution of the Navier–Stokes equations using first order slip velocity model [23]. This is expected because for Kn = 0.0194, the Knudsen layer plays a role in a very

Fig. 6 Pressure deviation from the linear pressure for outlet Knudsen number of 0.388 using different grid resolutions. Comparison of the TRT-LBE using Arlemark wall function with DSMC and IP results and first order slip Navier–Stokes solution of [23]
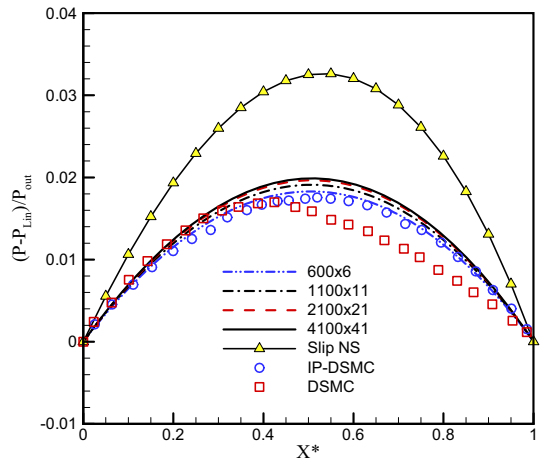
small region close to the wall surface. Therefore, the slip Navier–Stokes equations are still applicable in this Knudsen number. Consequently, it can be concluded that the present TRT-LBE converges to the slip Navier–Stokes solution at very low Knudsen numbers, as expected. For Kn = 0.194 (Fig. 5b), the maximum pressure deviations estimated by the exponential and Arlemark models are about 0.038 and 0.037, respectively. These values are in quite good agreement with the pressure deviation obtained by DSMC method, which is about 0.037. The maximum pressure deviation of the power law model is also about 0.039, which lies above the results of the exponential and Arlemark models. Furthermore, it can be observed that ψ_1 and ψ_2 models give a maximum pressure deviation of about 0.045, which is significantly higher than that of the DSMC method. However, they still provide better predictions rather than the standard LBE without considering wall distance functions, in which the maximum of pressure deviation is about 0.049.

In order to indicate the convergence behavior of the present model, the pressure distribution is obtained by using four different grid resolutions for the outlet Knudsen number of 0.388. In this part, the Arlemark wall function is implemented and the results of the simulation are compared against the analytical solution of the Navier–Stokes equations using first order slip velocity model as well as the results of the DSMC and IP-DSMC approaches. As illustrated in Fig. 6, the solution of the present LBE model converges under fine meshes. On the other hand, although the converged solution over predicts the maximum pressure deviation with respect to the DSMC and IP-DSMC data, it has significantly better prediction rather than the slip Navier–Stokes solution. It should be pointed out that the solution of the slip Navier–Stokes equations (in Figs. 5, 6) is obtained without using any improvement such as wall function implementation.

Velocity defect is another important parameter for modeling gas flows through micro-devices. This parameter, which exhibits the formation of Knudsen layer, can be calculated by:

$$\text{Velocity defect} = |U_{LBE} - U_{NS}| \tag{19}$$

which shows the difference between the slip velocity predicted by the TRT-LBE from that of the Navier–Stokes equations using first order slip velocity model near the wall of the channel. In Eq. (19) velocities are normalized by the maximum velocity at the centerline of the channel. According to Fig. 7, for low Knudsen numbers the velocity defect is small. This indicates that the effect of Knudsen layer is negligible at low Knudsen numbers. However, as

Fig. 7 Difference of slip velocity predicted by the TRT-LBE using different wall functions from solution of the slip Navier–Stokes equations [23]
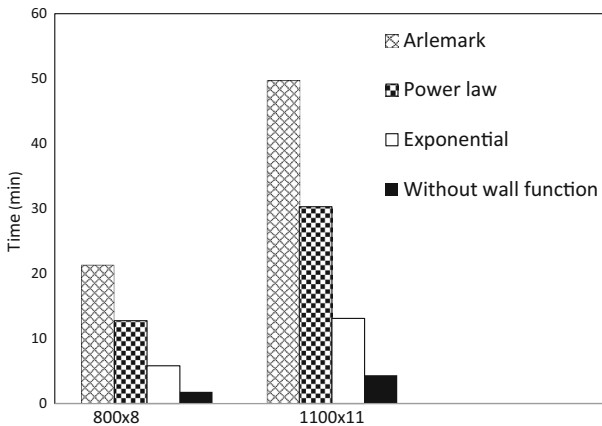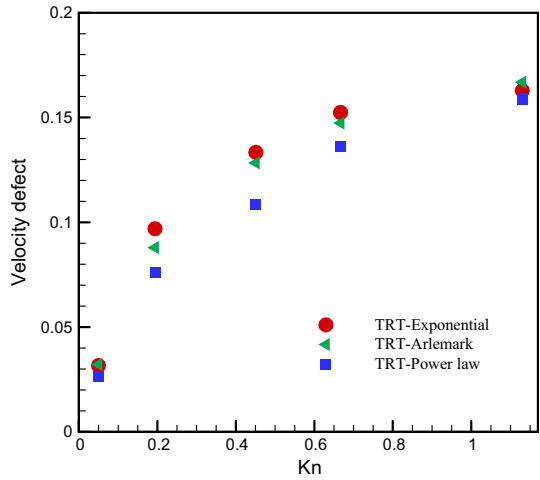

Fig. 8 Required computational time of the present TRT-LBE using different wall functions for different grid sizes at outlet Knudsen number of 5

the Knudsen number increases, the Knudsen layer plays a dominant role on the flow behavior and causes a relatively large velocity defect at the fluid-solid interface, as expected.

It has been shown up to this point that the exponential, Arlemark and power law wall functions provide the most accurate results among the examined wall functions. Clearly, implementation of wall functions increases the computational cost of the model. In this section, we aim to find how much the use of wall functions affects the overall computational performance of the TRT-LBE model. For this reason, the power law, Arlemark and exponential relations are applied to a micro/nano-channel with the outlet Knudsen number of Kn = 5. The performance of these expressions is evaluated with respect to the standard TRT model without using wall functions. The computations are done for two different lattice sizes 800×8 and 1100×11 on a system with Intel Core i5 CPU and 4 GB random access memory (RAM). The convergence criterion is fixed at $|(U_n - U_o)/U_o| < 10^{-6}$, where U is the average velocity at the outlet cross section of the channel and subscripts n and o represent the new and old time steps, respectively. Also, the initial values of the velocity and density are set to be $u = 0$ and $\rho = 1.5$, respectively. As can be seen from Fig. 8, the Arlemark model

is the most expensive relation. This model requires about 21 min to satisfy the convergence criterion for the coarse grid structure and about 49 min for the fine grid structure, which are about ten times higher than the standard TRT-LBE without using wall functions. However, the exponential model has a significantly better performance. This model increases the required computational time of the standard TRT model by about two times. Furthermore, the required computational time of the power law model is also higher than the standard LBE by about six times. It should be emphasized that the standard forms of the considered wall functions, which are available in the literature, are implemented in this study. These relations are obtained by using numerical integration with specific number of subintervals. Clearly, by using a different integration method or varying the number of subintervals one can implement these wall functions with different numerical efficiency. However, the above analysis attempts to indicate that the computational performance of the available wall functions can be widely different. Therefore, this parameter should also be taken into consideration in order to simulate micro/nano-gas flows using the wall function approach.

6 Conclusions

The lattice Boltzmann model with two relaxation times and based on the idea of wall function approach is employed in order to study rarefied gas flows in micro/nano-channels. Several available wall functions are implemented and evaluated from different viewpoints. The velocity profiles indicate that the Arlemark, power law and exponential models can significantly enhance the results obtained by the TRT-LBE up to Kn = 5. Beyond that, the accuracy of the existing wall distance functions begins to degrade. On the other hand, there is some disagreement between the mass flux predicted by the power law expression and reference data for Knudsen numbers higher than 1, while the exponential and Arlemark models can appropriately predict the mass flow behavior in the transition regime. Furthermore, the other implemented expressions (ψ_1 and ψ_2 models) are only applicable for the early transition flow regime (Kn ~ 0.1). Finally, a comparative study on the computational efficiency of the wall functions is performed, which indicates that the computational cost of the Arlemark model is rather expensive, while the exponential function provides significantly better computational efficiency. Overall, the exponential relation seems to be superior in terms of accuracy and computational efficiency among the considered wall function correlations. In addition, the applicability of the existing wall functions for Knudsen numbers higher than 5 is still questionable.

Compliance with Ethical Standards

Conflict of Interest   The authors declare that they have no conflict of interest.

References

1. Meng, J., Zhang, Y.: Accuracy analysis of high-order lattice Boltzmann models for rarefied gas flows. J. Comput. Phys. **230**(3), 835–849 (2011)
2. Shan, X., He, X.: Discretization of the velocity space in the solution of the Boltzmann equation. Phys. Rev. Lett. **80**(1), 65 (1998)

3. Ansumali, S., et al.: Hydrodynamics beyond Navier–Stokes: exact solution to the lattice Boltzmann hierarchy. Phys. Rev. Lett. **98**(14), 124502 (2007)
4. Kim, S.H., Pitsch, H., Boyd, I.D.: Accuracy of higher-order lattice Boltzmann methods for microscale flows with finite Knudsen numbers. J. Comput. Phys. **227**(22), 8655–8671 (2008)
5. Meng, J., et al.: Lattice ellipsoidal statistical BGK model for thermal non-equilibrium flows. J. Fluid Mech. **718**, 347–370 (2013)
6. Shan, X., Yuan, X.-F., Chen, H.: Kinetic theory representation of hydrodynamics: a way beyond the Navier–Stokes equation. J. Fluid Mech. **550**, 413–441 (2006)
7. Tang, G.-H., Zhang, Y.-H., Emerson, D.R.: Lattice Boltzmann models for nonequilibrium gas flows. Phys. Rev. E **77**(5), 046701 (2008)
8. Zhang, Y.-H., et al.: Capturing Knudsen layer phenomena using a lattice Boltzmann model. Phys. Rev. E **74**(5), 046704 (2006)
9. Stops, D.: The mean free path of gas molecules in the transition regime. J. Phys. D **3**(5), 685 (1970)
10. Guo, Z., Shi, B., Zheng, C.G.: An extended Navier–Stokes formulation for gas flows in the Knudsen layer near a wall. Europhys. Lett. **80**(2), 24001 (2007)
11. Xu, Z., Guo, Z.: Pressure distribution of the Gaseous flow in microchannel: a lattice Boltzmann study. Int. Commun. Heat Mass Transf. **14**, 1058–1072 (2013)
12. Arlemark, E.J., Dadzie, S.K., Reese, J.M.: An extension to the Navier–Stokes equations to incorporate gas molecular collisions with boundaries. J. Heat Transf. **132**(5), 041006 (2010)
13. Dongari, N., Zhang, Y., Reese, J.M.: Modeling of Knudsen layer effects in micro/nanoscale gas flows. Trans. ASME-I-J. Fluids Eng. **133**(9), 071101 (2011)
14. Dongari, N., et al.: The effect of Knudsen layers on rarefied cylindrical Couette gas flows. Microfluid. Nanofluid. **14**(1–2), 31–43 (2013)
15. Karniadakis, G.E., Becskèok, A., Aluru, N.R.: Microflows and Nanoflows, vol. 29. Springer, New York (2005)
16. Shokouhmand, H., Isfahani, A.H.M.: An improved thermal lattice Boltzmann model for rarefied gas flows in wide range of Knudsen number. Int. Commun. Heat Mass Transf. **38**(12), 1463–1469 (2011)
17. Li, Q., et al.: Lattice Boltzmann modeling of microchannel flows in the transition flow regime. Microfluid. Nanofluid. **10**(3), 607–618 (2011)
18. Michalis, V.K., et al.: Rarefaction effects on gas viscosity in the Knudsen transition regime. Microfluid. Nanofluid. **9**(4–5), 847–853 (2010)
19. Bahukudumbi, P.: A unified engineering model for steady and quasi-steady shear-driven gas microflows. Microscale Thermophys. Eng. **7**(5), 291–315 (2003)
20. Dongari, N., Sharma, A., Durst, F.: Pressure-driven diffusive gas flows in micro-channels: from the Knudsen to the continuum regimes. Microfluid. Nanofluid. **6**(5), 679–692 (2009)
21. Toschi, F., Succi, S.: Lattice Boltzmann method at finite Knudsen numbers. Europhys. Lett. **69**(5), 549 (2005)
22. Luo, L.-S.: Comment on "discrete Boltzmann equation for microfluidics". Phys. Rev. Lett. **92**(15), 139401–139401 (2004)
23. Nie, X., Doolen, G.D., Chen, S.: Lattice-Boltzmann simulations of fluid flows in MEMS. J. Stat. Phys. **107**(1–2), 279–289 (2002)
24. Verhaeghe, F., Luo, L.-S., Blanpain, B.: Lattice Boltzmann modeling of microchannel flow in slip flow regime. J. Comput. Phys. **228**(1), 147–157 (2009)
25. Suga, K., Ito, T.: On the multiple-relaxation-time micro-flow lattice boltzmann method for complex flows. Comput. Model. Eng. Sci. **75**, 141–172 (2011)
26. Suga, K., et al.: Evaluation of a lattice Boltzmann method in a complex nanoflow. Phys. Rev. E **82**(1), 016701 (2010)
27. Esfahani, J.A., Norouzi, A.: Two relaxation time lattice Boltzmann model for rarefied gas flows. Physica A **393**(1), 51–61 (2014)
28. Norouzi, A., Esfahani, J.A.: Two relaxation time lattice Boltzmann equation for high Knudsen number flows using wall function approach. Microfluid. Nanofluid. **18**(2), 323–332 (2015)
29. Guo, Z., Zheng, C., Shi, B.: Lattice Boltzmann equation with multiple effective relaxation times for gaseous microscale flow. Phys. Rev. E Stat. Nonlinear Soft Matter Phys. **77**(3 Pt 2), 036707 (2008)
30. Liu, X., Guo, Z.: A lattice Boltzmann study of gas flows in a long micro-channel. Comput. Math. Appl. **65**(2), 186–193 (2013)
31. Talon, L., et al.: Assessment of the two relaxation time lattice-Boltzmann scheme to simulate Stokes flow in porous media. Water Resour. Res. **48**(5), W04526 (2012)
32. Lockerby, D.A., Reese, J.M., Gallis, M.A.: The usefulness of higher-order constitutive relations for describing the Knudsen layer. Phys. Fluids **17**(12), 100609 (1994-present)

33. Guo, Z., Zhao, T., Shi, Y.: Physical symmetry, spatial accuracy, and relaxation time of the lattice Boltzmann equation for microgas flows. J. Appl. Phys. **99**(9), 074903 (2006)
34. Dongari, N., Zhang, Y., Reese, J.M.: Molecular free path distribution in rarefied gases. J. Phys. D **44**(14), 125502 (2011)
35. Ansumali, S., Karlin, I.V.: Kinetic boundary conditions in the lattice Boltzmann method. Phys. Rev. E **66**(2), 026311 (2002)
36. Succi, S.: Mesoscopic modeling of slip motion at fluid-solid interfaces with heterogeneous catalysis. Phys. Rev. Lett. **89**(8), 064502–064502 (2002)
37. Suga, K.: Lattice Boltzmann methods for complex micro-flows: applicability and limitations for practical applications. Fluid Dyn. Res. **45**(3), 034501 (2013)
38. Shen, C., Fan, J., Xie, C.: Statistical simulation of rarefied gas flows in micro-channels. J. Comput. Phys. **189**(2), 512–526 (2003)